ARMA 20–1158

SAND2020-4286C

Analysis of Hydraulic Fracturing on the 4100 Level at the Sanford Underground Research Facility

Ingraham, M.D., and Schwering, P.C.
Sandia National Laboratories, Albuquerque, NM, USA
Burghardt, J.
Pacific Northwest National Laboratory, Richland, WA, USA
Ulrich, C.
Lawrence Berkeley National Laboratory, Berkeley, CA, USA
Doe, T.
tdoegeo, Redmond, WA, USA
Roggenthen, W.M. and Reimers, C.
South Dakota School of Mines & Technology, Rapid City, SD, USA
The EGS Collab Team

ABSTRACT: A series of hydrofractures were performed on the 4100 ft. level of the Sanford Underground Research Facility (SURF) to quantify the minimum principal stress and stress orientation. The motivation for this work was to determine the suitability of the site as a second testbed for the EGS Collab project and to inform the testbed design. EGS Collab is a meso-scale project where experiments are being performed to increase permeability in low-permeability rock and improve our understanding of appropriate techniques and models required for developing enhanced geothermal systems. In order to design the second testbed, a ~50 m vertical HQ (96 mm) pilot borehole was drilled in June, 2019, to perform a series of mini-frac tests to determine the rock stress state. Utilizing an elastic model based on the ISIP (Instantaneous Shut In Pressure), testing indicates that the minimum principal stress is 20.4 MPa oriented NNE (24°) and plunges at an angle of approximately 28°.

1. INTRODUCTION

As part of determining a location for Experiment 2 of the EGS Collab project (Kneafsey et al. 2018), a 50 m vertical HQ (96 mm) borehole was drilled on the 4100 level of the Sanford Underground Research Facility (SURF), the borehole is located in an alcove near the Yates shaft (Heise, 2015). This borehole was to be used for a series of tests to determine the feasibility of the location for shear fracture stimulation as part of the Experiment 2 test protocol. As part of the testing, a series of hydraulic fractures were performed throughout the length of the borehole. These were used to determine the minimum principal stress and infer stress direction from the comparison of pre- and post-test borehole logs.

2. ROCK STRUCTURE

The rock in question is part of the Yates unit, a heavily folded and metamorphosized amphibolite (Caddey et al., 1991, Hart et al., 2014). This is contrary to the rock type which was used for Experiment one which was the Poorman formation (Oldenburg et al., 2017, Vigilante et al., 2017, Wang et al., 2017), a layer of schist which overlays and the Yates amphibolite. Both formations are steeply dipping, so that even though the tests described here occur at a shallower depth than Experiment one, they are in an underlying formation.

Throughout the Yates formation there are a number of rhyolite layers. The borehole used for this work intersected three of them, two of which were relatively thin, on the order of 10's of centimeters. The third however is on the order of 10 m thick and results in significant modification of the local stress state. The rhyolite layers can be identified in the core, and it is highly apparent in the borehole gamma logs, as well as in the sonic logs. Typically, the rhyolite is also visible in the optical televiewer logs, and in the core it is usually (but not always) much lighter in color as compared with the dark amphibolite. However, the amphibolite also has quartz veins running through it which in the optical logs should not be confused with the rhyolite.

Initial core inspection, impression packer measurements, and geophysical wireline logging results, which included optical and acoustic televiewer, fluid temperature conductivity, and full waveform sonic, show a complex package of rock that primarily consists of amphibolite (dominant) and 10 m of rhyolite; that has frequent, mostly healed, calcite and quartz fractures with a few open fractures.

Pre-test wireline log results indicated that the temperature of the well increased from approximately 20° C to 25° C

Sandia National Laboratories is a multimission laboratory managed and operated by National Technology & Engineering Solutions of Sandia, LLC, a wholly owned subsidiary of Honeywell International Inc., for the U.S. Department of Energy's National Nuclear Security Administration under contract DE-NA0003525.

along the length of the well. Conductivity of the native water in the well was found be approximately 8300 µS/cm. The gamma log was useful in conjunction with the optical televiewer and comparison to core in identifying the rhyolite zones. Sonic logs indicated that the rock is strong with a P-wave velocity of around 5300 m/s and a S-wave velocity of approximately 4700 m/s in the amphibolite. In the large rhyolite zone these drop to 3200 and 2900 m/s respectively.

3. EQUIPMENT/PROCEDURE

The hydraulic fracturing was performed using a straddle packer with an interval of 1.1 meters. The system used to perform the fractures was an air driven hydraulic pump which was instrumented with multiple pressure transducers and an inlet flow meter. Valving was implemented to allow for independent control of the packer and interval pressures, note that interval pressure was measured on a static return line to eliminate flow induced pressure loss and help remove the cyclic noise from the pump. Typical fracture procedure involved setting the packer at the desired depth measure on the wireline, inflating the packers, and then injecting at a constant rate of approximately 0.5 lpm. Once the breakdown pressure was reached the injection continued to a total volume of approximately 3 liters and was then shut in. After a shut-in period of approximately 3 minutes the interval was allowed to flow back. Typically, this cycle was repeated 2-3 times to investigate reopening behavior, but this work will only look at the first cycle of the injection. An example of a complete injection (Lee and Haimson, 1989, Haimson, 1993) is shown below in Figure 1.

Prior to running any of the fracture experiments wireline logs were performed on the hole including: fluid temperature, conductivity, optical and acoustic televiewer, and full waveform sonic. Figure 2 shows the logs for the entire well with the fracture locations noted. After the fracture tests were performed the acoustic televiewer log was repeated, and impressions were taken of the fracture locations. Figure 3 shows the acoustic televiewer results from one of the fracture locations. In general because of the dark color of the rock and the small fractures generated the optical televiewer did not produce good results, so the acoustic televiewer data was the primary diagnostic used for determining fracture orientation. The results from the impression packer did not show anything significantly different from the acoustic televiewer (Lee and Haimson, 1989).

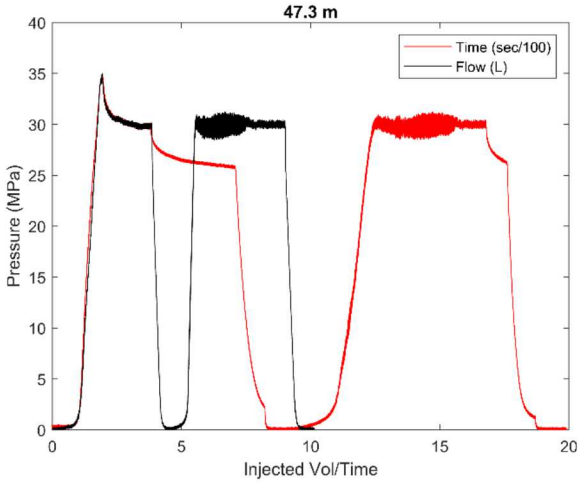

Fig. 1. Time and Injected Volume history for a fracture performed at 47.3 m.

4. RESULTS/DISCUSSION

The test operation went smoothly, and reasonable injection curves were obtained for all of the selected test locations (Figure 4 shows the first injection cycle for each location). In general, the tests performed in the amphibolite illustrated a textbook breakdown curve. Some of the curves were flatter than expected, considering how tight the rock is, with little difference between the fracture initiation and breakdown. However, it appears that in these cases the test reopened a natural fracture that was not completely healed instead of generating a new fracture. These distinctions were difficult to observe comparing the pre and posttest televiewer logs, as the fractures (reopening of a healed fracture or newly generated) were very difficult to see in the logs and core photos, the fracture orientations reported in Table 1 are from measurements of fractures observed on the posttest televiewer log. As the test zone approached the rhyolite it was also observed that the fracture initiation pressure decreased along with the ISIP (Instantaneous Shut In Pressure), however, the breakdown was still typical of what is seen in other parts of the amphibolite (Table 1). Tests in the rhyolite were significantly lower across the board in terms of pressure and did not illustrate a peaked fracture breakdown. Re-entering the amphibolite below the rhyolite zone a dramatic increase in pressures (initiation, breakdown, and ISIP) were seen. It is suspected that the more compliant rhyolite is generating a stress heterogeneity in the region in and around the rhyolite. Thus, the amphibolite below the rhyolite zone is carrying a larger portion of the load. Figure 5 shows a plot of the data presented in Table 1, showing the effect of the depth and different rock types on fracture initiation, breakdown pressure, and ISIP.

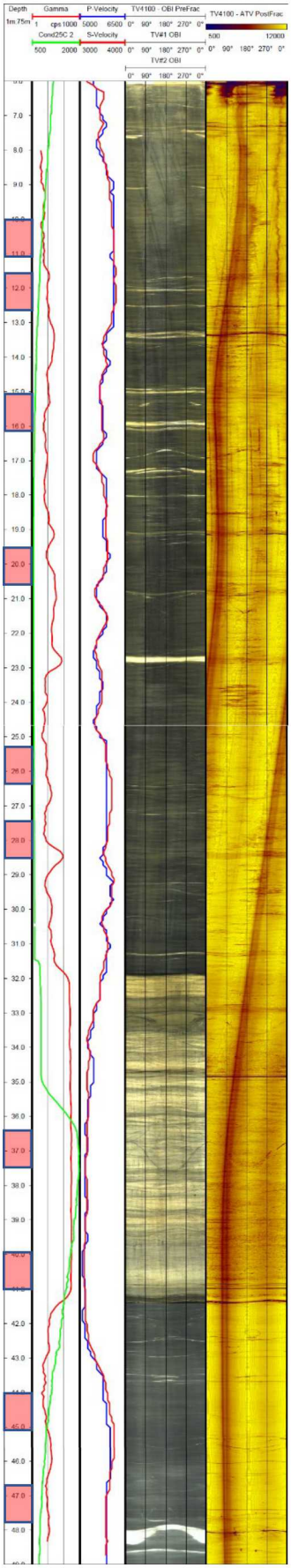

Fig. 2. Logs of Gamma/Conductivity, P/S-Wave velocity, optical televiewer, and acoustic televiewer from the borehole in question. Note that the fracture locations are marked on the depth scale with red boxes.

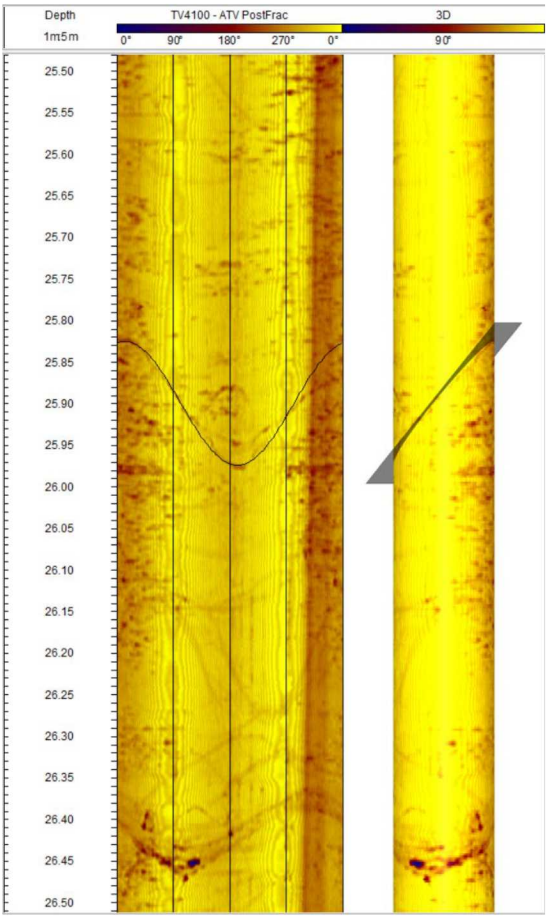

Fig. 3. Example of a pick from the acoustic televiewer logs. This is the fracture performed at 25.7 m.

Examination of the data in Table 1 in detail, shows that the pressure data and the fracture orientations fall into 3 categories. One in the amphibolite above the rhyolite zone, the large rhyolite zone, and the amphibolite below the rhyolite zone. In general, the orientations of the fractures, but not the fracture pressures, are similar in each of these zones. Note that the two shallowest fractures were excluded from the analysis of the stress and stress orientation, this was done because the fractures could not be located in the shallowest (10.2 m) interval, and the confidence in the pick in the second shallowest (12.1 m) interval was low.

The plots of the observed fractures and fracture angles are shown in Figure 6 on a lower hemisphere projection stereonet plot, with poles indicated as dots. In general, all of the points show the same general trend, however, as with the pressures, they tend to group into 3 sections: above, within and below the large rhyolite layer, and again the top two fractures were excluded from the analysis. The plots are grouped by color, where the red

plots show above the rhyolite, the green are within the rhyolite and blue are below the rhyolite.

Using an elastic model to estimate the minimum principal stress (as laid out by Haimson, 1993), the tests performed throughout the length of the hole provide a minimum principal stress of approximately 21.8 MPa which strikes at 16 degrees NNE, with a plunge of 23 degrees. However, if one takes the rhyolite and the amphibolite below the rhyolite as a stress inhomogeneity and excluding the data from the tests closest to the top of the hole where fracture orientation were unclear, it changes the minimum principal stress to be 21.5 MPa oriented at 24 degrees NNE with a plunge of 28 degrees. While these are not huge differences they could be significant when developing the second test bed. Also, in comparing the results of this work with that performed during the kISMET project (Oldenburg et al. 2017, Wang et al. 2017), the stress orientation and inclination are not greatly different. That experiment found that the minimum principal stress was 21.7 MPa, with an orientation of the minimum compressive stress of N 2° E (corrected for magnetic north, Kneafsey and others, 2020) plunging at 9 degrees. The vertical stress is approximately 35.4 MPa (Pariseau, 1986) on the 4100 level of the SURF. The intermediate principal stress was not determined as part of this work, but based off other work at SURF, it is not unreasonable to assume it is close to the vertical stress.

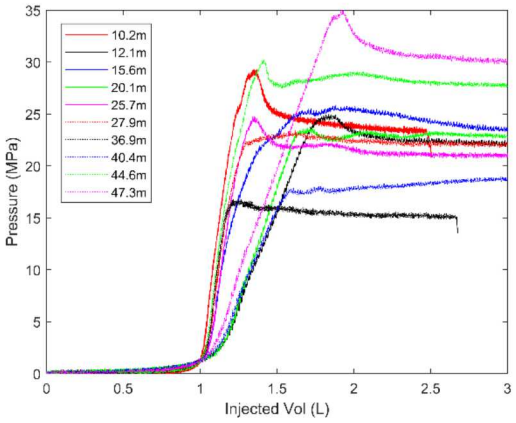

Fig. 4. Pressure vs injected volume curves for all of the fractures, note that they were all aligned so that the pressure rise began at 1 liter injected volume.

5. CONCLUSIONS

The presence of the rhyolite in this rock formation caused a fair amount of uncertainty in the determination of the minimum principal stress, and its direction. The tests in and just above the rhyolite demonstrated an approximately 30% reduction in breakdown when compared with those performed in the amphibolite away from the rhyolite. Tests in the amphibolite below the rhyolite required about 30+% higher pressure to achieve breakdown compared to the amphibolite above the rhyolite.

This resulted in the question of which data to utilize for the analysis considering the desires of the project. It was determined that for the project we would attempt to stay above the rhyolite zone and were therefore most interested in the results for the stress in that area. Utilizing the tests performed above the rhyolite zone, we find the average strike of induced hydraulic fractures to be 114° with an average dip of 62°. Utilizing an elastic model based off the ISIP this indicates that the minimum principal stress is 21.5 MPa oriented NNE (24° Azimuth), and plunges at an angle of approximately 28°.

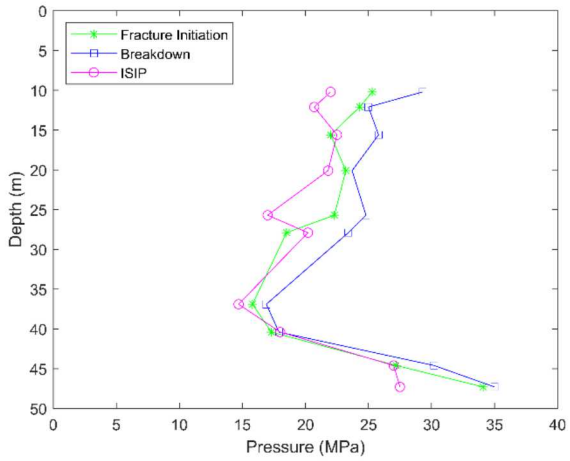

Fig. 5. Pressure vs depth for fractures performed in the test hole. Note the decrease in the fracture pressure in the rhyolite (37 and 40 m fractures, and then the increase in pressure at the toe of the well, below the rhyolite.

Table 1. Table showing results of fracture tests, note pressures are in MPa and angles are measured in degrees. For the test performed at 10.2 m there was no clear fracture visible on the televiewer log. Tests performed in the rhyolite zone are illustrated with blue text. Data in red text was omitted from the analysis due to uncertainty in the fracture picks.

Interval Center	Fracture Initiation	Break-down	ISIP	Strike from True North	Dip
10.2	25.1	29.3	22.3	?	?
12.1	23.8	25.0	21.5	131	56
15.6	21.8	25.8	22.7	117	59
20.1	22.4	23.7	21.7	117	68
25.7	23.4	24.8	20.0	110	59
27.9	22.1	23.4	21.5	111	63
36.9	15.6	16.9	15.0	111	84
40.4	17.4	17.9	18.0	103	79
44.6	26.6	30.2	27.1	91	66
47.3	33.6	35.0	28.5	88	60

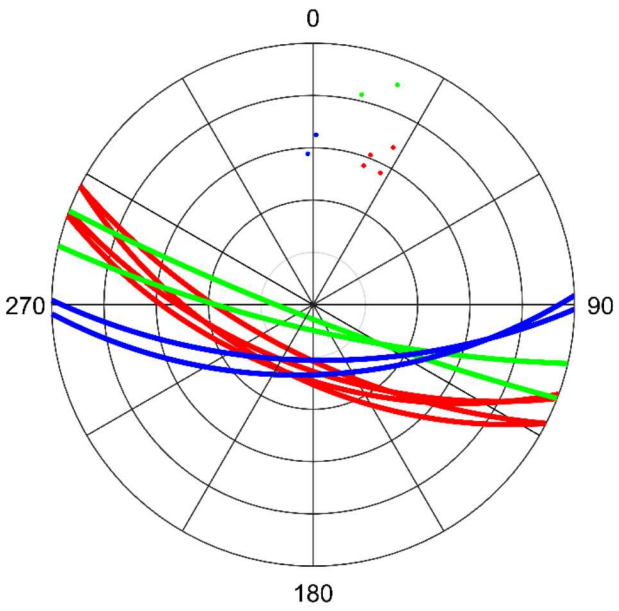

Fig. 6. Stereonet projection of the induced fractures, red shows fractures above the rhyolite zone, green within the rhyolite, and blue below the rhyolite.

ACKNOWLEDGEMENTS

The authors would like to acknowledge the support of the entire EGS Collab team, but specifically Taylor Myers and Joe Pope who assisted in performing the fracture tests and post test logging. We would also like to thank Moo Lee for the critical review of the work.

The research supporting this work took place in whole or in part at the Sanford Underground Research Facility in Lead, South Dakota. This research was also supported by the U.S. Department of Energy, Office of Energy Efficiency and Renewable Energy (EERE), Geothermal Technologies Office (GTO). The assistance of the Sanford Underground Research Facility and its personnel in providing physical access and general logistical and technical support is acknowledged.

The EGS Collab Team consists of: J. Ajo-Franklin, T. Baumgartner, K. Beckers, D. Blankenship, A. Bonneville, L. Boyd, S. Brown, S.T. Brown, J.A. Burghardt, T. Chen, Y. Chen, K. Condon, P.J. Cook, D. Crandall, P.F. Dobson, T. Doe, C.A. Doughty, D. Elsworth, J. Feldman, A. Foris, L.P. Frash, Z. Frone, P. Fu, K. Gao, A. Ghassemi, H. Gudmundsdottir, Y. Guglielmi, G. Guthrie, B. Haimson, A. Hawkins, J. Heise, M. Horn, R.N. Horne, J. Horner, M. Hu, H. Huang, L. Huang, K.J. Im, M. Ingraham, R.S. Jayne, T.C. Johnson, B. Johnston, S. Karra, K. Kim, D.K. King, T. Kneafsey, H. Knox, J. Knox, D. Kumar, K. Kutun, M. Lee, K. Li, Z. Li, R. Lopez, M. Maceira, P. Mackey, N. Makedonska, C.J. Marone, E. Mattson, M.W. McClure, J. McLennan, T. McLing, C. Medler, R.J. Mellors, E. Metcalfe, J. Miskimins, J. Moore, C.E. Morency, J.P. Morris, S. Nakagawa, G. Neupane, G. Newman, A. Nieto, C.M. Oldenburg, W. Pan, T. Paronish, R. Pawar, P. Petrov, B. Pietzyk, R. Podgorney, Y. Polsky, S. Porse, B.Q. Roberts, M. Robertson, W. Roggenthen, J. Rutqvist, D. Rynders, H. Santos-Villalobos, M. Schoenball, P. Schwering, V. Sesetty, C.S. Sherman, A. Singh, M.M. Smith, H. Sone, F.A. Soom, C.E. Strickland, J. Su, D. Templeton, J.N. Thomle, C. Ulrich, N. Uzunlar, A. Vachaparampil, C.A. Valladao, W. Vandermeer, G. Vandine, D. Vardiman, V.R. Vermeul, J.L. Wagoner, H.F. Wang, J. Weers, J. White, M.D. White, P. Winterfeld, T. Wood, S. Workman, H. Wu, Y.S. Wu, Y. Wu, E.C. Yildirim, Y. Zhang, Y.Q. Zhang, Q. Zhou, M.D. Zoback

Sandia National Laboratories is a multimission laboratory managed and operated by National Technology and Engineering Solutions of Sandia LLC, a wholly owned subsidiary of Honeywell International Inc. for the U.S. Department of Energy's National Nuclear Security Administration under contract DE-NA0003525.

SAND2020-XXXX C

REFERENCES

1. Caddey, S.W., L. Bachman, T.J. Campbell, R.R. Reid, and R.P. Otto. 1991. The Homestake Gold Mine, An Early Proterozoic Iron-Formation-Hosted Gold Deposit, Lawrence County, South Dakota, U. S. Geological Survey Bulletin 1857-J, Geology and Resources of Gold in the United States, 67 pp.
2. Haimson, B.C. 1993. The Hydraulic Fracturing Method of Stress Measurement: Theory and Practice. In *Rock Testing and Site Characterization*, ed. J.A. Hudson, 395-412.
3. Hart, K., Trancynger, T.C., Roggenthen, W., and Heise, J. "Topographic, geologic, and density distribution modeling in support of physics experiments at the Sanford Underground Research Facility (SURF)." *Proceedings of the South Dakota Academy of Science*, 93, (2014), 33-41.
4. Heise, J. "The Sanford Underground Research Facility at Homestake."Journal of Physics: Conference Series,v. 606(1), IOP Publishing, (2015).
5. Kneafsey, T.J., P. Dobson, D. Blankenship, J. Morris, H. Knox, P. Schwering, M. White, T. Doe, W. Roggenthen, E. Mattson, R. Podgorney, T. Johnson, J. Ajo-Franklin, C. Vallado, and the EGS Collab Team. 2018. In *Proceedings of the 43rd Workshop on Geothermal*

Reservoir Engineering, Stanford, CA, 12-14 February 2018.

6. Kneafsey, T. J., D. Blankenship, P. F. Dobson ,J. P. Morris, M. D. White, P. Fu, P. C. Schwering, J.B. Ajo-Franklin, L. Huang, Martin Schoenball, T. C. Johnson, H. A. Knox, G. Neupane, J. Weers, R. Horne, Y. Zhang, W. Roggenthen, T. Doe, E. Mattson, C. Valladao, and the EGS Collab team, 2020, The EGS Collab Project: Learnings from Experiment , SGP-TR-216, Proceedings, 45th Workshop on Geothermal Reservoir Engineering Stanford University, Stanford, California. February 10-12, 2020.

7. Lee, M.Y., and B.C. Haimson. 1989. Statistical Evaluation of Hydraulic Fracturing Stress Measurement Parameters. *Int. J. Rock Mech. Min. Sci.*26:6: 447-456.

8. Oldenburg, C.M., Dobson, P.F., Wu, Y., Cook, P.J., Kneafsey, T.J., Nakagawa, S., Ulrich, C., Siler, D.L., Guglielmi, Y., Ajo-Franklin, J., Rutqvist, J., Daley, T.M., Birkholzer, J.T., Wang, H.F., Lord, N.E., Haimson, B.C., Sone, H., Vigilante, P., Roggenthen, W.M., Doe, T.W., Lee, M.Y., Ingraham, M., Huang, H., Mattson, E.D., Zhou, J., Johnson, T.J., Zoback, M.D., Morris, J.P., White, J.A., Johnson, P.A., Coblentz, D.D., and Heise, J. "Hydraulic fracturing experiments at 1500 m depth in a deep mine: Highlights from the kISMETproject."Proceedings, 42nd Workshop on Geothermal Reservoir Engineering, Stanford University, (2017),9 p.

9. Pariseau, W.G. (1986). Research study on pillar design for vertical crater retreat (vcr) mining. *USBM OFR,* 44-86.

10. Vigilante, P.J., H. Sone, H.F. Wang, B. Haimson, and T.W. Doe. 2017. Anisotropic Strength of Poorman Formation Rocks, kISMET Project. In *Proceedings of the 51st U.S. Rock Mechanics/Geomechanics Symposium, San Francisco, 25-28 June 2017*.

11. Wang, H.F., M.Y. Lee, T.W. Doe, B.C. Haimson, and P.F. Dobson. 2017. In-Situ Stress Measurement at 1550-Meters Depth at the kISMET Test Site in Lead, S.D. In *Proceedings of the 51st U.S. Rock Mechanics/Geomechanics Symposium, San Francisco, 25-28 June 2017*.